Dyes and Pigments 83 (2009) 328–333

Contents lists available at ScienceDirect

Dyes and Pigments

journal homepage: www.elsevier.com/locate/dyepig

The synthesis and characterization of photonic materials composed of substituted fluorene donors and a porphyrin acceptor

Neeraj Agarwal*

Department of Chemical Sciences, Tata Institute of Fundamental Research, Homi Bhabha Road, Colaba, Mumbai 400005, India

ARTICLE INFO

Article history:
Received 3 March 2009
Received in revised form
19 May 2009
Accepted 20 May 2009
Available online 2 June 2009

Keywords:
Porphyrin
Fluorene
Fluorescence
Energy transfer
Thin-film
Aggregation

ABSTRACT

Three novel porphyrin derivatives namely 5,10,15,20-tetra-[7-cyanophenyl-9,9’-bis-(2-ethylhexyl)fluoren-2-yl]-porphyrin, 5,10,15,20-tetra-[7-(4-acetylphenyl)-9,9’-bis-(2-ethylhexyl)fluoren-2-yl]-porphyrin and 5,10,15,20-tetra-[7-pyrenyl-9,9’-bis-(2-ethylhexyl)fluoren-2-yl]-porphyrin were synthesized. Substitution of the aryl groups on the *meso*-fluorene using Suzuki-Miyaura coupling enabled a study to be undertaken of the energy transfer from the *meso* fluorenyl to the porphyrin core. To calculate the extent of energy transfer, the corresponding model fluorene compounds 7-cyanophenyl-9,9’-bis-(2-ethylhexyl)fluorene, 7-acetylphenyl-9,9’-bis-(2-ethylhexyl)fluorene and 7-pyrenyl-9,9’-bis-(2-ethylhexyl)fluorene were also synthesized. Fluorescence studies of both the porphyrin derivatives and model compounds showed efficient energy transfer occured from the aryl-fluorene donor to the porphyrin acceptor. Upon excitation, due to energy transfer, a characteristic porphyrin emission was observed at ~656 nm; ~99% energy transfer in solution was observed in these donor–acceptor systems. Thin-film emission results indicate a low degree of aggregation in the donor–acceptor systems.

1. Introduction

Development of organic and polymeric light-emitting diodes has become an active area of research. Organic light-emitting diodes (OLEDs) have potential use in the large-area flat panel displays due to their high brightness, low operation voltage, and cost-effective solution processability [1–4]. Essentially, blue, green, and red colors are required to develop a full colour display. Green emitters [5,6] have already been achieved with high brightness and efficiency, which meet the requirements for commercial applications. Performance of blue emitters is not as efficient as of green and the main problems are their stabilities and lifetimes [7,8]. Red light-emission in OLEDs is usually achieved by doping the red dyes. The most widely used red emitters are heavy metal complexes [9–12], and Pt(II) porphyrins [13,14], among which octaethylporphyrin Pt(II) [15] is commonly used with host materials such as AlQ3 or poly-(9,9-dioctylfluorene-2,7-diyl)s (POFs). When a phosphorescent dopant is used, an optimum concentration of the dopant (5–10%) is required. The higher doping concentration causes aggregation in solid state which usually leads to self-quenching of emission and results in lower efficiency for the devices [16]. Also it was found that low concentration of dopant generally causes incomplete energy transfer from host to dopant [15].

Energy transfer (ET) between a donor (D) and acceptor (A) usually involves components of both Forster and Dexter processes [17]. However, in conjugated materials, the Dexter exchange mechanism is usually limited to a short distance (<10 Å). ET from a donor to acceptor decreases exponentially with donor to acceptor distance. Recent findings suggest that efficient energy transfer is achieved in cases with properly aligned singlet state [18]. While such D-A systems are of fundamental interest, their solid-state photonic properties are of practical importance for fabrication of OLEDs. However, incomplete energy transfer in D-A systems, having blue emitting donors and red emitting acceptors, may lead to emission in broad visible region and hence could provide the white light source for OLEDs.

In OLEDs, efficient energy transfer from host to guest material in low concentration of guest molecules is required. Photoluminescence properties, including through bond energy transfer, of well-defined porphyrin–fluorene oligomers based materials are established in the literature [19]. However, the preparation of these materials, having oligo-fluorene arms on the *meso* position of porphyrin, requires several synthetic steps and tedious purification methods. These difficulties limit their use as the material of choice in OLEDs. For practical applications, a low-cost large-scale synthesis is urgently required. Here, we report a simple approach to synthesize the star-shaped porphyrin–fluorene derivatives **1–3** (Fig. 1). Substituents on

---

* Tel.: +91 22 22782864; fax: +91 22 22804610.
E-mail address: nagarwal@tifr.res.in

0143-7208/$ – see front matter © 2009 Elsevier Ltd. All rights reserved.
doi:10.1016/j.dyepig.2009.05.011

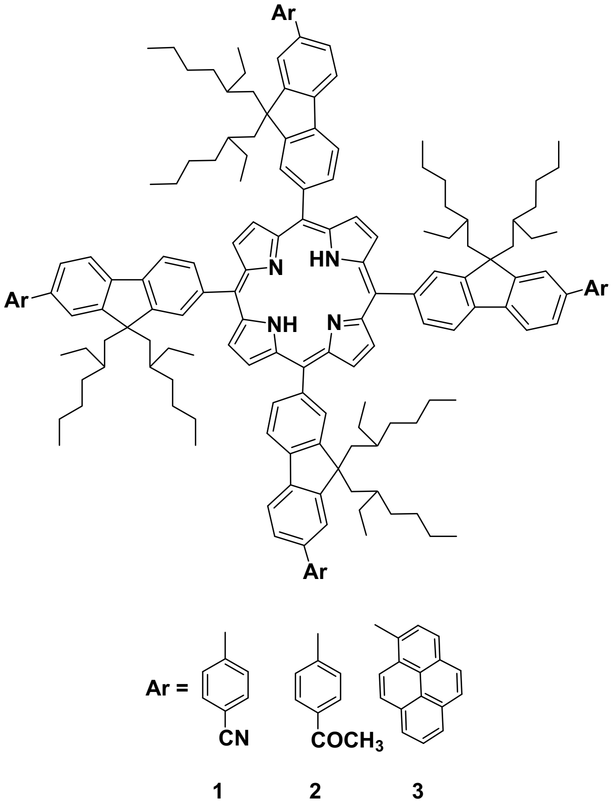

Fig. 1. Porphyrin derivatives **1**–**3**.

the *meso*-fluorene arms of porphyrin were varied. The absorption and photophysical properties were investigated and an efficient energy transfer was observed. 2-Aryl fluorene model compounds were also synthesized to calculate the extent of energy transfer.

2. Experimental

2.1. Materials and instruments

All solvents and K_2CO_3, were obtained from SD Fine Chemicals (India). Anhydrous dimethylformamide, 2,7-dibromo-9,9'-(2-ethylhexyl)fluorene, pyrrole, trifluoracetic acid, 2,3-dichloro-5,6-dicyanobenzoquinone, aryl boronic acids and tris(dibenzylideneacetone) dipalladium(0) ($Pd_2(dba)_3$) were purchased from Sigma–Aldrich and used as received. Tetrakis(triphenylphosphine)palladium(0) ($Pd(PPh_3)_4$) was freshly prepared. Reactions that require anhydrous conditions were carried out under inert atmosphere of nitrogen in oven-dried glasswares. Tetrahydofuran was dried over Na wire and distilled under nitrogen. 7-Bromo-9,9'-(2-ethylhexyl)fluorene-2-carbaldehyde (**4**) was synthesized according to the previously reported method [14,19]. Progress of reaction was monitored using Silica Gel TLC plates by UV detection (254 and 365 nm). Silica gel was used for column chromatography. Melting points (uncorrected) were checked using a capillary melting point apparatus. ^1H and ^{13}C NMR spectra were recorded using Bruker spectrometer with working frequency 500 MHz for ^1H NMR and 125 MHz for ^{13}C NMR. For ^1H NMR and ^{13}C NMR, the chemical shifts were referenced to $CHCl_3$ present as impurity in the deuterated solvent, $CDCl_3$. Mass spectra were measured using a Thermo Finnigan LCQ Deca Electrospray quadrupole ion trap mass spectrometer (Thermo Electron Co., Hemel Hempstead, Herts, UK) or on MALDI-TOF (Micromass Tof Spec 2E). Photoluminescence was measured using SPEX Fluorolog 1681.

2.2. Synthesis

*2.2.1. Synthesis of 5,10,15,20-tetra-[7-bromo-9,9'-bis-(2-ethylhexyl)fluoren-2-yl]-porphyrin (**5**)*

A stream of argon was passed through dichloromethane (300 ml) in a 500 ml round-bottomed flask for 10 min. Compound **4** (2.0 g, 4.05 mmol) and pyrrole (0.30 ml, 4.27 mmol) were added and argon purging was continued for an additional 10 min. Trifluoroacetic acid (0.50 ml) was added and the reaction mixture was stirred for 1 h. DDQ (0.91 g, 4.00 mmol) was then added and the reaction mixture was stirred in open air for an additional 1.5 h. The solvent was removed under reduced pressure and the crude compound was purified by silica column using CH_2Cl_2. The desired compound **5** was obtained as a purple solid. Yield: 1.05 g (12%); M. P. > 250 °C; ^1H NMR ($CDCl_3$, δ in ppm): 8.80 (s, 8H, β-pyrrole), 8.21 (s, 8H), 8.04 (s, 4H), 7.79–7.82 (m, 4H), 7.58–7.64 (m, 8H), 2.09 (s, 16H, CH_2), 0.62–1.01 (m, 120H) −2.66 (s, 2H, NH); ^{13}C NMR ($CDCl_3$, δ in ppm): 153.51, 153.48, 149.26, 146.37, 141.08, 140.82, 133.49, 132.01, 131.04, 130.24, 127.57, 121.41, 121.39, 120.56, 117.92, 117.89, 55.60, 45.06, 45.04, 45.03, 35.15, 33.69, 33.67, 33.58, 28.28, 28.27, 27.73, 22.87, 14.14, 10.90, 10.88, 10.86, 10.11, 10.07; MALDI-TOF calcd for $C_{136}H_{170}N_4Br_4$: 2180.45, Found: 2181.8.

*2.2.2. Synthesis of porphyrin derivatives **1**–**3***

In a reaction vessel, bromoporphyrin **5** (0.022 g, 0.01 mmol), K_2CO_3 (0.014 g, 0.1 mmol), aryl boronic acid (0.06 mmol), tri-(*o*-tolyl)-phosphine (0.002 g, 0.007 mmol) and $Pd_2(dba)_3$ (0.003 mg) were dissolved in THF–water mixture and stirred under nitrogen atmosphere. The reaction mixture was refluxed at 75 °C for 24 h. The reaction progress was monitored by TLC. Upon completion of the coupling the solvent was evaporated and the crude compound was purified by column chromatography to obtain the pure compounds **1**–**3** as purple solids in 65–76% yield.

*2.2.2.1. 5,10,15,20-Tetra-[7-cyanophenyl-9,9'-bis-(2-ethylhexyl)fluoren-2-yl]-porphyrin (**1**).* Yield: 0.016 g (70%); M. P. > 250 °C; FT-IR (KBr): 2230 cm^{-1}; ^1H NMR ($CDCl_3$, δ in ppm): 8.90 (s, 8H, β-pyrrole), 8.33 (s, 8H), 8.13 (s, 4H), 8.10 (d, 4H, $J = 7.9$ Hz), 7.73–7.87 (m, 16H), 7.77 (d, 8H, $J = 7.2$ Hz), 2.24 (s, 16H, CH_2), 0.96–1.02 (m, 72H), 0.71 (s, 48H, CH_3), −2.49 (s, 2H, NH); ^{13}C NMR ($CDCl_3$, δ in ppm): 152.1, 149.4, 146.2, 143.4, 143.2, 141.8, 141.7, 141.1, 140.2, 137.7, 134.7, 132.7, 132.5, 130.4, 128.9, 128.3, 127.7, 127.5, 125.4, 125.4, 120.5, 119.1, 119.0, 110.6, 55.4, 55.3, 35.2, 35.1, 33.6, 31.9, 29.7, 29.3, 28.9, 28.3, 27.7, 26.4, 22.9, 22.7, 14.0, 10.8; MALDI-TOF calcd for $C_{164}H_{186}N_8$: 2267.48, Found: 2267.91.

*2.2.2.2. 5,10,15,20-Tetra-[7-acetylphenyl-9,9'-bis-(2-ethylhexyl) fluoren-2-yl]-porphyrin (**2**).* Yield: 0.019 g (76%); M. P: >250 °C; FT-IR (KBr): 1675 cm^{-1}; ^1H NMR ($CDCl_3$, δ in ppm): 8.86 (s, 8H, β-pyrrole), 8.21–8.27 (br m, 8H), 8.10 (d, 12H, $J = 8.3$ Hz), 8.05 (d, 4H, $J = 8.0$ Hz), 7.82 (d, 8H, $J = 8.2$ Hz), 7.76 (d, 8H, $J = 7.6$ Hz), 2.67 (s, 12H, acetyl), 2.20 (s, 16H, CH_2), 0.89–1.05 (m, 72H), 0.67 (s, 48H, CH_3), −2.54 (s, 2H, NH); ^{13}C NMR ($CDCl_3$, δ in ppm): 197.82, 151.95, 146.41, 143.30, 141.48, 141.39, 140.99, 140.38, 138.50, 138.45, 135.69, 134.78, 130.50, 130.29, 129.25, 129.05, 128.96, 128.41, 127.48, 127.40, 127.25, 127.15, 126.59, 126.48, 125.40, 123.01, 120.63, 120.55, 120.44, 118.09, 55.44, 45.01, 44.97, 43.00, 35.10, 29.70, 28.31, 26.75, 22.81, 14.04, 10.85; MALDI-TOF calcd for $C_{168}H_{198}N_4O_4$: 2335.54, Found: 2335.95.

*2.2.2.3. 5,10,15,20-Tetra-[7-pyrenyl-9,9'-bis-(2-ethylhexyl)fluoren-2-yl]-porphyrin (**3**).* Yield: 0.017 g (65%); M. P: >250 °C; FT-IR (KBr): 3046 cm^{-1}; ^1H NMR ($CDCl_3$, δ in ppm): 8.95 (s, 8H, β-pyrrole), 8.05–8.34 (m, 52H, aromatic), 7.74 (s, 8H, aromatic), 2.20 (s, 16H, CH_2), 0.91–1.09 (m, 72H), 0.75 (s, 48H, CH_3), −2.52 (s, 2H, NH); ^{13}C NMR

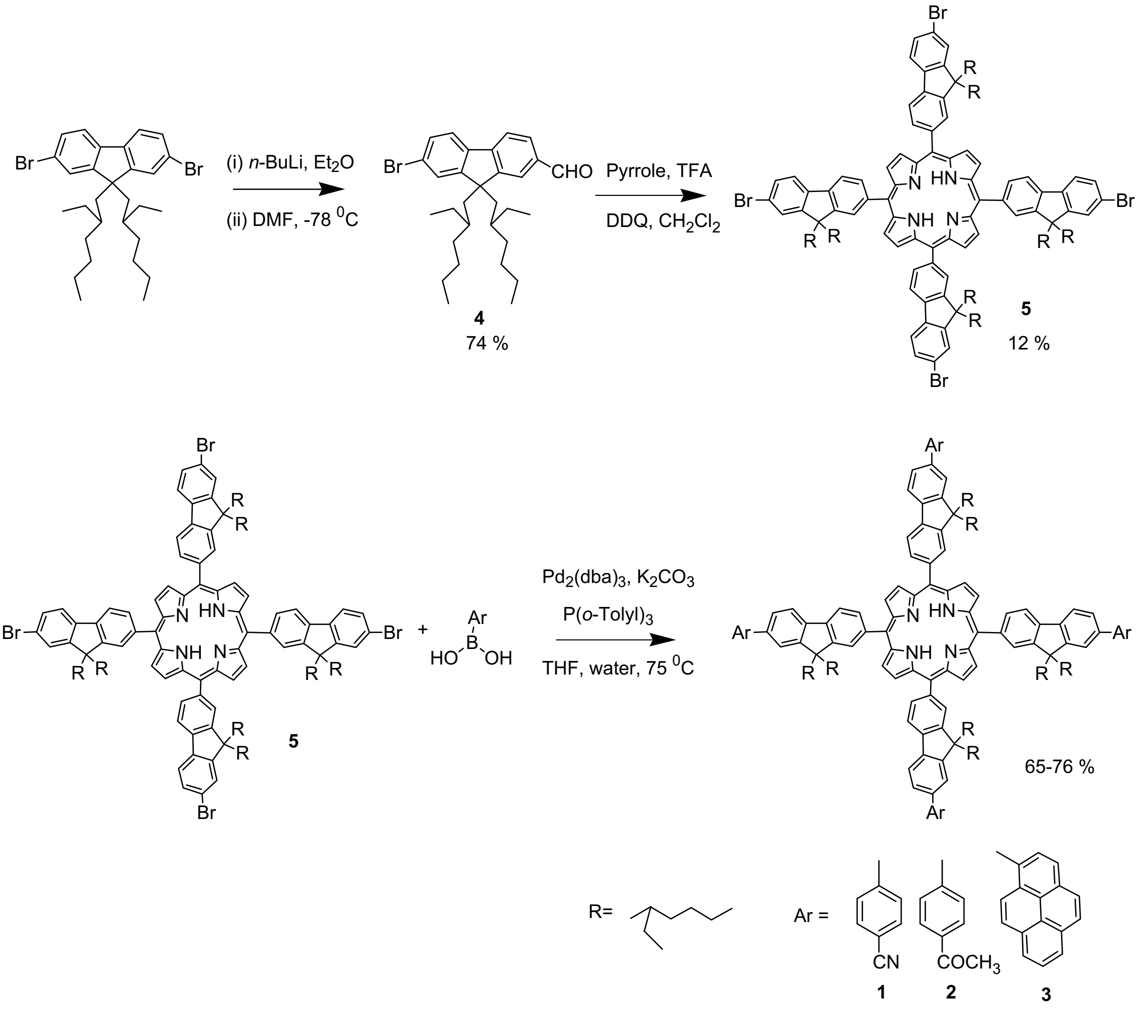

Fig. 2. Schematic representation of synthesis of porphyrin derivatives **1**–**3**.

(CDCl$_3$, δ in ppm): 151.6, 149.9, 149.2, 148.6, 141.2, 141.7, 141.1, 140.6, 140.4, 140.0, 139.9, 138.5, 131.5, 137.1, 130.6, 130.1, 129.6, 129.1, 128.7, 127.7, 127.4, 127.0125.0, 124.6, 120.7, 120.0, 117.9, 117.2, 55.4, 45.3, 34.6, 34.4, 34.0, 29.7, 28.9, 28.3, 27.6, 26.7, 23.0, 13.1, 9.8; MALDI-TOF calcd for $C_{200}H_{206}N_4$: 2663.62, Found: 2663.57.

2.2.3. *Synthesis of model compounds, **6**–**8***

In a reaction vessel, 2,7-Dibromo-9,9'-(2-ethylhexyl)fluorene (0.58 g, 1.0 mmol), K_2CO_3 (1.38 g, 10.0 mmol), aryl boronic acid (1.1 mmol), and $Pd_2(PPh_3)_4$ (0.1 mmol) were dissolved in DME–water mixture. The reaction mixture was refluxed under nitrogen atmosphere for 20 h. The reaction progress was monitored by TLC. Upon completion of the coupling the solvent was evaporated and the crude compound was purified by column chromatography to obtain the pure compounds **6**–**8** as viscous liquids in 60–73% yield.

*2.2.3.1. 7-Cyanophenyl-9,9'-bis-(2-ethylhexyl)fluorene (**6**).* Yield: 0.39 g (73%) FT-IR (KBr): 2227 cm^{-1}; ^{1}H NMR (CDCl$_3$, δ in ppm): 7.69–7.78 (m, 6H), 7.54–7.59 (m, 4H), 7.47 (d, 1H, $J = 8.0$ Hz), 1.96–2.07 (m, 4H, CH$_2$), 1.27 (s, 2H, CH), 0.71–0.93 (m, 16H, CH$_2$), 0.50–0.60 (m, 12H, CH$_3$); ^{13}C NMR (CDCl$_3$, δ in ppm): 153.00, 151.10, 146.04, 140.89, 139.39, 137.71,

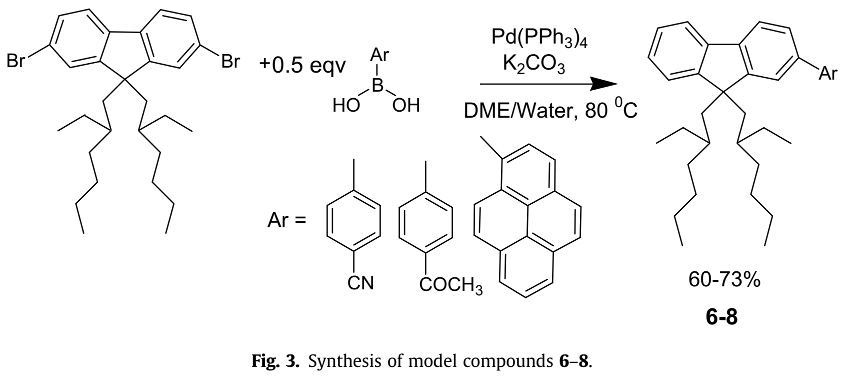

Fig. 3. Synthesis of model compounds **6**–**8**.

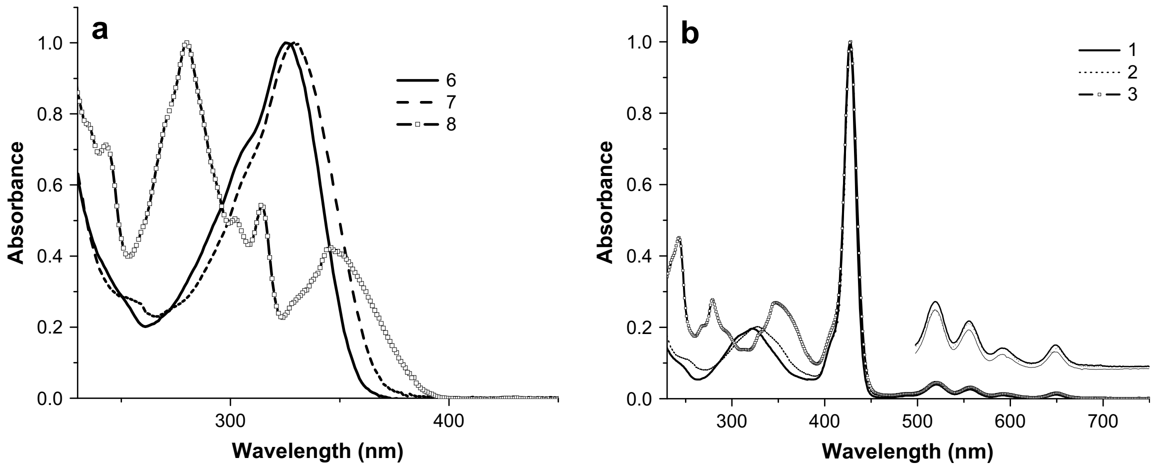

Fig. 4. Peak normalized absorption spectra of (a) **6–8** and (b) **1–3** in CH_2Cl_2.

132.70, 130.09, 127.68, 127.52, 127.43, 126.38, 122.79, 122.69, 121.10, 119.01, 110.67, 55.33, 44.28, 34.69, 33.72, 28.06, 27.06, 22.70, 13.92, 10.36; MALDI-TOF calcd for $C_{36}H_{45}N$: 492.12, Found: 492.12.

*2.2.3.2. 7-Acetylphenyl-9,9'-bis-(2-ethylhexyl)fluorene (**7**).* Yield: 0.34 g (62%) FT-IR (KBr): 1673 cm^{-1}; ^{1}H NMR (CDCl$_3$, δ in ppm): 8.05 (d, 2H, $J = 8.15$ Hz), 7.75 (d, 1H, $J = 8.45$ Hz), 7.71 (d, 2H, $J = 8.15$ Hz), 7.58–7.60 (m, 2H), 7.57 (s,1H), 7.54–7.47 (m, 3H), 2.64 (s, 3H, CH_2), 1.95–2.08 (m, 4H, CH_2), 1.27 (s, 2H, CH), 0.73–0.93 (m, 16H, CH_2), 0.51–0.61 (m, 12H, CH_3); ^{13}C NMR (CDCl$_3$, δ in ppm): 197.72, 153.05, 150.89, 150.83, 146.20, 140.46, 139.59, 138.43, 135.69, 130.00, 128.91, 127.08, 122.89, 121.19, 120.90, 107.50, 55.29, 44.29, 34.67, 28.06, 27.05, 22.71, 14.02, 10.34; MALDI-TOF calcd for $C_{37}H_{48}O$: 508.37, Found: 509.25.

*2.2.3.3. 7-Pyrenyl-9,9'-bis-(2-ethylhexyl)fluorene (**8**).* Yield: 0.35 g (60%) ^{1}H NMR (CDCl$_3$, δ in ppm): 8.16–8.25 (m, 4H), 8.10–8.12 (t, 2H), 7.96–8.04 (m, 3H), 7.83 (d, 1H, $J = 7.5$ Hz), 7.62–7.66 (m, 2H), 7.55–7.60 (m,3H), 7.50 (d, 1H, $J = 8.0$ Hz), 1.97–2.00 (m, 4H, CH_2), 1.25 (s, 2H, CH), 0.58–0.98 (m, 28H, alkyl); ^{13}C NMR (CDCl$_3$, δ in ppm): 166.20, 155.97, 152.76, 152.36, 139.96, 139.14, 134.92, 134.41, 134.26, 133.89, 131.49, 130.05, 127.35, 127.30, 121.03, 120.89, 109.01, 107.50, 55.34, 44.28, 34.64, 33.54, 27.98, 27.02, 22.70, 14.00, 10.30.

3. Results and discussion

3.1. Synthesis and characterization

Porphyrin derivatives **1–3** were synthesized as outlined in Fig. 2. 7-Bromo-9,9'-(2-ethylhexyl)fluorene-2-carbaldehyde (**4**) was synthesized [14] by the reaction of 2,7-dibromo-9,9'-(2-ethylhexyl)fluorene with 1.2 equivalents of *n*-BuLi followed by the addition of 1.2 equivalents of dry dimethylformamide at −78 °C. Purification by column chromatography gave **4** in ~74% yield. In ^{1}H NMR, signal at 10.07 ppm was assigned corresponding to one proton of aldehyde group in **4**. The condensation of **4** and pyrrole (1.1 eq) in dichloromethane catalyzed by TFA and followed by the oxidation using DDQ resulted in the formation of the dark crude product which was neutralized by the addition of few drops of triethylamine. Column chromatography purification of the crude product afforded the purple colored bromoporphyrin, **5** in 12% yields. In ^{1}H NMR, singlet at −2.70 ppm is due to inner NH of the pyrrole, a singlet accounting for eight protons of the β-pyrroles at 8.76 ppm and characteristic signals of fluorene alkyl chains were observed. Suzuki-Miyaura coupling [20] of bromoporphyrin **5**, with aryl boronic acid(s) catalyzed by $Pd_2(dba)_3$ in basic medium produced the compounds **1–3** in good yields along with the mono, di and tri substituted products. All the newly synthesized compounds were characterized and studied by several spectroscopic techniques.

Model fluorene compounds, 2-(*p*-cyanophenyl)-9,9'-(2-ethylhexyl)-fluorene, **6**,2-(*p*-acetophenyl)-9,9'-(2-ethylhexyl)-fluorene, **7** and 2-pyrenyl-9,9'-(2-ethylhexyl)-fluorene, **8** were synthesized as shown in Fig. 3. 2,7-Dibromo-9,9'-(2-ethylhexyl)-fluorene was cross-coupled with 0.5 eq of aryl boronic acid using $Pd(PPh_3)_4$, K_2CO_3 in aq. DME and heated under reflux at 80 °C for 16–18 h under nitrogen. 2-Aryl (major) and 2,7-diaryl-fluorene (minor) derivatives were formed. Model compounds **6–8** were purified by column chromatography using hexanes and ethyl acetate as eluent and were characterized by several spectroscopic techniques.

3.2. Optical properties

The UV–vis absorption spectra of **1–3** and model compound **6–8** are shown in Fig. 4. Compound **1–3** showed features of both porphyrin and fluorene chromophores. The π–π^* absorption at ~324 nm in **1**, **2** and at 345 nm in **3** originates from the presence of the 2-aryl-fluorene fragments. The soret band at ~427 nm and Q-bands at ~520, 557, 593 and 649 nm were observed. Compound **3** showed an additional absorption at 280 nm which is due to the pyrene unit. Model compounds **6** and **7** show intense absorption at ~327 nm. Compound **8** shows red shift in absorption at 346 nm due to the increase in conjugation by the presence of pyrenyl group. No significant shift was observed in Soret and Q bands of

Table 1
Photophysical parameters of **1–3** and **5**.

Compound	Absorbance nm (log ε)	λ_{em} (nm)
1	650 (4.17), 593 (4.19), 555 (4.40), 520 (4.51), 427 (5.73), 322 (5.09)	656, 719
2	651 (3.97), 593 (3.84), 556 (4.25), 520 (4.32), 428 (5.75), 327 (5.12)	656, 720
3	648 (4.04), 590 (4.09), 556 (4.33), 519 (4.39), 428 (5.61), 348 (5.22), 279 (5.31)	657, 718
5	650 (4.12), 592 (4.09), 553 (4.31), 518 (4.41), 425 (5.69)	

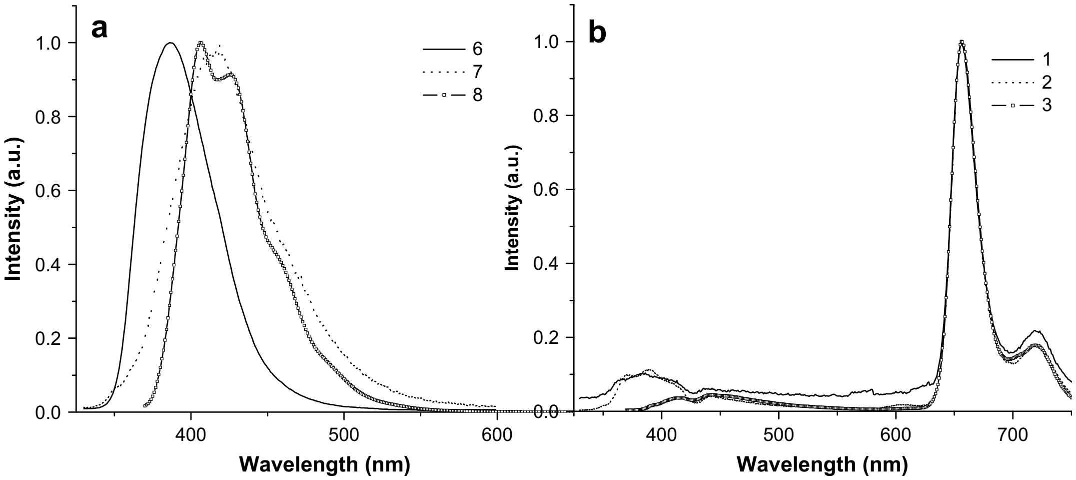

Fig. 5. Peak normalized emission spectra of (a) **6–8** and (b) **1–3** in CH_2Cl_2.

porphyrins **1**–**3**, compared to **5**. Absorption peaks and extinction coefficients for **1**–**3** are summarized in Table 1.

Fluorescence spectra of **1**–**3** and model compounds, **6**–**8** were recorded in dichloromethane. Compound **6** showed emission peak at 386 nm when excited at 315 nm. Emission of **6** significantly overlaps with Soret band of the porphyrin and hence fulfills the first condition for energy transfer. A molecular model of **1** generated by Hyperchem [21] suggests that the distance between fluorene and porphyrin is within the limits of Dexter energy transfer (<10 Å). Excitation of **1** at 315 nm shows emission at 657 and 720 nm, which are the characteristic features of porphyrin emission. These emission features indicate the energy transfer from fluorene donor to porphyrin acceptor. Emission spectra of **1**–**3** and **6**–**8** are shown in Fig. 5. Excitation scan (λ_{em} at 657 nm) of **1**–**3** show the features of both porphyrin and fluorene units, which further confirm the energy transfer from fluorene to porphyrin. The extent of ET was calculated by using the following formula.

$$\phi_{\mathrm{ET}} = 1 - \frac{A_{\mathrm{d}}}{A_{\mathrm{da}}}\frac{I_{\mathrm{da}}}{I_{\mathrm{d}}}$$

where, ϕ_{ET} is the energy transfer efficiency, A_{da} is the absorbance of donor–acceptor compound, A_{d} is the absorbance of donor in the absence of acceptor, I_{da} is the emission intensity of donor–acceptor compound and I_{d} is the emission intensity of donor in absence of acceptor. Compound **1** and **2** show 99% and 83% energy transfer (λ_{em} at 386 nm for **1** and 419 nm for **2**), respectively, when excited at 315 nm. Compound **3** shows 99% energy transfer (λ_{em} at 406 nm) when excited at 350 nm.

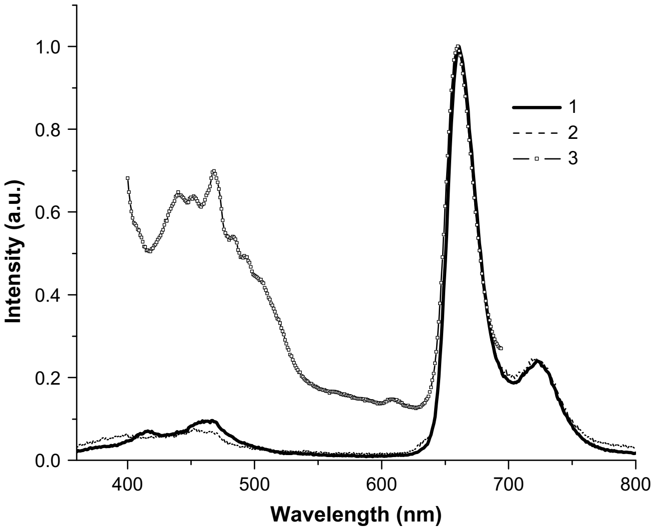

Fig. 6. Peak normalized emission spectra of **1**–**3** in thin films.

To make practical use of organic materials it is important to study their fluorescence in thin films. Fluorescence spectra of porphyrin **1**–**3** in thin films were recorded and are shown in Fig. 6. Compounds **1**–**3** showed prominent emission peaks at 660 nm and 720 nm while emission from fluorene component is weak in **1** and **2** which show the efficient energy transfer from fluorene to porphyrin core. In the case of **3** emission from pyrenyl–fluorene unit is not significantly suppressed indicating less energy transfer in the thin film. The residual emission in blue region may be due to the inefficient energy transfer from pyrene to fluorene to porphyrin. However, the emission properties of **3** in the thin film need to be explored in more detail to assess its application for white light in OLEDs. A very small red shift of ∼4 nm, with respect to solution emission maxima of 1–3, was observed. These observations suggest a low aggregation of **1**–**3** in thin films. Presumably the alkyl chains on the fluorene units prevent the molecules stacking and hence results in low aggregation [19].

4. Conclusion

In conclusion, new donor–acceptor composites of porphyrin and aryl substituted-fluorene were synthesized and characterized. Photophysical studies of these porphyrin derivatives show efficient energy transfer from fluorene to porphyrin core. Model fluorene compounds were also synthesized to quantify the energy transfer. Thin film emission spectra of these donor–acceptor materials show minimal degree of aggregation.

Acknowledgments

Author thanks Prof. N. Periasamy for helpful discussions. The national facility for high field NMR at TIFR is acknowledged for NMR spectra.

References

[1] Shinar J. Organic light-emitting devices. New York: Springer-Verlag; 2003.
[2] Muller DC, Falcou A, Reckefuss N, Rojahn M, Wlederhirm V, Rudati P, et al. Multi-colour organic light-emitting displays by solution processing. Nature 2003;421(6925):829–33.

[3] Burroughes JH, Bradley DDC, Brown AB, Marks RN, Mackay K, Friend RH, et al. Light emitting diodes based on conjugated polymers. Nature 1990;347(6293): 539–41.

[4] Baldo MA, Thompson ME, Forrest SR. High-efficiency fluorescent organic light-emitting devices using a phosphorescent sensitizer. Nature 2000;403(6771): 750–3.

[5] Kawamura Y, Goushi K, Brooks J, Brown JJ, Sasabe H, Adachi C. 100% Phosphorescence quantum efficiency of Ir(III) complexes in organic semiconductor films. Applied Physics Letters 2005;86(7). 071104.

[6] Carter JC, Grizzi I, Heeks SK, Lacey DJ, Latham SG, May PG, et al. ,. Operating stability of light-emitting polymer diodes based on poly(*p*-phenylene vinylene). Applied Physics Letters 2005;71(1):34–6.

[7] Chan L, Lee R, Hsieh C, Yeh H, Chen C. Optimization of high-performance blue organic light-emitting diodes containing tetraphenylsilane molecular glass materials. Journal of the American Chemical Society 2002;124(22):6469–79.

[8] Tao S, Lee CS, Lee S-T, Zhanga X. Efficient blue and white organic light-emitting devices based on a single bipolar emitter. Applied Physics Letters 2007;91(1). 013507.

[9] Kido J, Hayase H, Hongawa K, Nagai K, Okuyama K. Bright red light-emitting organic electroluminescent devices having a europium complex as an emitter. Applied Physics Letters 1994;65(17):2124–6.

[10] Kappaun S, Sax S, Eder S, Moller KC, Waich K, Niedermair F, et al. 8-Quinolinolates as ligands for luminescent cyclometalated iridium complexes. Chemistry of Materials 2007;19(6):1209–11.

[11] Agarwal N, Nayak PK. Synthesis, characterization, photophysical and electrochemical properties of new phosphorescent dopants for OLEDs. Tetrahedron Letters 2008;49(17):2710–3.

[12] Lamansky S, Djurovich P, Murphy D, Abdel-Razzaq F, Lee H-E, Adachi C, et al. Highly phosphorescent bis-cyclometalated iridium complexes: synthesis, photophysical characterization, and use in organic light emitting diodes. Journal of the American Chemical Society 2001;123(18):4304–12.

[13] Kwong RC, Sibley S, Dubovoy T, Baldo M, Forrest SR, Thompson ME. Efficient, saturated red organic light emitting devices based on phosphorescent platinum(II) porphyrins. Chemistry of Materials 1999;11(12):3709–13.

[14] Montes VA, Perez-Bolıvar C, Agarwal N, Shinar J, Anzenbacher Jr P. Molecular-wire behavior of OLED materials: exciton dynamics in multichromophoric Alq$_3$–oligofluorene–Pt(II) porphyrin triads. Journal of the American Chemical Society 2006;128(38):12436–8.

[15] Baldo MA, O'Brien DF, You Y, Shoustikov A, Sibley S, Thompson ME, et al. Highly Efficient Phosphorescent Emission from Organic Electroluminescent Devices. Nature 1998;395:151–4.

[16] Baldo MA, O'Brien DF, Thompson ME, Forrest SR. Excitonic singlet-triplet ratio in a semiconducting organic thin film. Physics Review B 1999;60(20):14422–8.

[17] Lakowicz JR. Principles of fluorescence spectroscopy. Kluwer Academics/ Plenum publishers; 1999.

[18] Tinnefeld P, Heilemann M, Sauer M. Design of molecular photonic wires based on multistep electronic excitation transfer. Physical Chemistry and Chemical Physics 2005;6(2):217–22.

[19] Li B, Li J, Fu Y, Bo Z. Porphyrins with four monodisperse oligofluorene arms as efficient red light-emitting materials. Journal of the American Chemical Society 2004;126(11):3430–1.

[20] Miyaura N. Metal-catalyzed cross-coupling reactions. In: De Meijere A, Diederich F, editors. Weinheim: Wiley-VCH; 2004.

[21] Calculations were performed using semi-empirical method with Hyperchem AM1.